HHS Public Access

Author manuscript

Mol Cancer Ther. Author manuscript; available in PMC 2017 June 01.

Published in final edited form as:

Mol Cancer Ther. 2016 June ; 15(6): 1163–1176. doi:10.1158/1535-7163.MCT-15-0973.

A novel plant sesquiterpene lactone derivative DETD-35 suppresses BRAF^{V600E} mutant melanoma growth and overcomes acquired vemurafenib resistance in mice

Jia-Hua Feng[1,2], **Kyoko Nakagawa-Goto**[3,4], **Kuo-Hsiung Lee**[4], and **Lie-Fen Shyur**[1,5,*]

[1]Agricultural Biotechnology Research Center, Academia Sinica, Taipei 115, Taiwan

[2]Institute of Plant Biology, College of Life Science, National Taiwan University, Taipei 106, Taiwan

[3]College of Medical, Pharmaceutical and Health Sciences, Kanazawa University, Kakuma-machi, Kanazawa 920-1192, Japan

[4]Natural Products Research Laboratories, Eshelman School of Pharmacy, University of North Carolina, Chapel Hill, North Carolina 27599, USA

[5]PhD Program in Translational Medicine, College of Medicine, Kaohsiung Medical University, Kaohsiung 708, Taiwan

Abstract

Acquired resistance to vemurafenib develops through reactivation of RAF/MEK/ERK signaling or bypass mechanisms. Recent combination therapies such as a MEK inhibitor combined with vemurafenib show improvement in major clinical end points but the percentage of patients with adverse toxic events is higher than with vemurafenib monotherapy and most patients ultimately relapse. Therefore, there is an urgent need to develop new anti-melanoma drugs and/or adjuvant agents for vemurafenib therapy. In this study, we created a novel semi-organically modified derivative, DETD-35, from deoxyelephantopin (DET), a plant sesquiterpene lactone demonstrated as an anti-inflammatory and anti-mammary tumor agent. Our results show that DETD-35 inhibited proliferation of a panel of melanoma cell lines, including acquired vemurafenib resistance A375 cells (A375-R) established in this study, with superior activities to DET and no cytotoxicity to normal melanocytes. DETD-35 suppressed tumor growth and reduced tumor mass as effectively as vemurafenib in A375 xenograft study. Furthermore, DETD-35 also reduced tumor growth in both acquired (A375-R) and intrinsic (A2058) vemurafenib resistance xenograft models, where vemurafenib showed no anti-tumor activity. Notably, the combination of DETD-35 and vemurafenib exhibited the most significant effects in both *in vitro* and *in vivo* xenograft studies due to synergism of the compound and the drug. Mechanistic studies suggested that DETD-35 overcame acquired vemurafenib resistance at least in part through deregulating MEK-ERK, Akt, and STAT3 signaling pathways and promoting apoptosis of cancer cells. Overall, our results

[*]**Corresponding Author:** Lie-Fen Shyur, Agricultural Biotechnology Research Center, Academia Sinica, No. 128, Sec. 2, Academia Road, Nankang, Taipei 115, Taiwan. Tel./Fax.: +886-2-26515028; ; Email: lfshyur@ccvax.sinica.edu.tw

Conflict of interests

The authors declare no conflict of interests.

suggest that DETD-35 may be useful as a therapeutic or adjuvant agent against $BRAF^{V600E}$ mutant and acquired vemurafenib resistance melanoma.

Keywords

RAF inhibitor; DETD-35; drug resistance; melanoma/skin cancers; novel antitumor agent

Introduction

Melanoma is the most lethal form of skin cancer and cases are increasing year by year. In the United States, the estimated number of new melanoma cases in 2001 was 51,400. This figure grew by 43.7% to 73,873 cases in 2015 ([1], [2]). Mutation in BRAF, V-raf murine sarcoma viral oncogene homolog B1 protein, $BRAF^{V600E}$ is found in approximately 50% of melanoma patients and drives RAF/MEK/ERK mitogen-activated protein kinase (MAPK) signaling to promote cancer progression ([3]). Therefore, a number of inhibitors targeting BRAF mutation or MAPK signaling have been developed. For example, vemurafenib (PLX4032), a small molecule specifically targeting $BRAF^{V600E}$ mutation, was discovered by Plexxikon in 2008 ([4]), and received FDA approval for treatment of late-stage melanoma in 2011 due to its promising clinical efficacy. Unfortunately, patients developed drug resistance and eventually relapsed within an average of 7 months after vemurafenib therapy ([5]). Acquired resistance to PLX4032 in human melanoma was mainly through paradoxical activation of MAPK signaling or bypass mechanisms ([6]–[11]). The reactivation of MEK-ERK signaling is driven by either a RAF-independent pathway through overexpression of MAP kinase 8 (MAP3K8, or COT) or the activation of the receptor tyrosine kinases (RTKs) ([12]–[14]). RTK signaling is initially suppressed by the elevated state of ERK-dependent feedback in $BRAF^{V600E}$ mutant melanoma cells in which RAS activity is low and $BRAF^{V600E}$ functions as a monomer. Upon vemurafenib treatment, inhibition of ERK activity relieves ERK-dependent feedback and allows ligand-dependent signaling by growth factors, leading to a rebound in RAS activity that promotes the formation of RAF dimers and reactivation of MEK-ERK signaling despite the presence of vemurafenib ([15]). These findings led to clinical trials such as a MEK inhibitor combined with vemurafenib or other BRAF inhibitors ([16]). Nonetheless, although recent combination therapy showed improvement in major clinical end points, the percentage of patients with adverse toxic events are higher than with vemurafenib monotherapy and most patients ultimately relapse ([16]–[18]). Therefore, it is important to continue to develop new anti-melanoma drugs and/or novel adjuvant approaches for vemurafenib therapy.

Elephantopus scaber L. is a traditional Chinese medicine which has been used for various inflammation-related syndromes. Our laboratory has isolated a bioactive compound deoxyelephantopin (DET) from *E. scaber* which shows anti-inflammation, hepatoprotective and anti-breast cancer activities by modulating multiple mechanisms, such as activation of the JNK-mediated apoptotic pathways, deregulation of the IKK/NFκB pathway and the ubiquitin proteasome machinery, and impeding TS/A cell motility by inhibiting calpain-mediated adhesion dynamics and inducing reactive oxygen species and aggresome formation ([19]–[22]). Based on a structural modeling analysis, we previously observed that the specific

carbonyl group at C12, C15 and C16 of DET directly interacts with RelA subunit of NF-κB through inter-hydrogen bonding. This interaction between DET and RelA likely averts the RelA subunit from binding to its DNA target ([20]). Notably, DET is also observed to be superior to paclitaxel (PTX) in prolonging the lifespan/survival rate in TS/A mammary tumor isograft bearing mice ([19]). In addition, DET has been reported to possess anti-lung adenocarcinoma ([23]), nasopharyngeal carcinoma ([24]) and human lymphocyte proliferation *in vitro* and anti-ascites tumor *in vivo* ([25]). Together, we consider DET as a novel lead compound for further modification or optimization of its structure to create a more potent drug lead for cancer management. We have thus initiated semi-organic synthesis of DET derivatives (DETDs) in order to obtain a potent DETD for melanoma treatment.

In this report, we provide a comprehensive evaluation of the preclinical activity profile of DETD-35, a derivative of DET, in $BRAF^{V600E}$ mutant and acquired vemurafenib resistance melanoma cells *in vitro* and *in vivo*. DET and vemurafenib were also evaluated in parallel. We showed that DETD-35 effectively inhibited $BRAF^{V600E}$ mutant and acquired vemurafenib resistance xenograft tumor growth in mice, with superior activities to parental compound DET. The synergism of DETD-35 and vemurafenib led to better *in vitro* and *in vivo* efficacy compared to treatment with either agent alone. This study demonstrates the novel therapeutic potential of DETD-35 against $BRAF^{V600E}$ mutant and acquired vemurafenib resistance in melanoma.

Materials and Methods

Preparation of DET and organic synthesis of DETDs

DET isolation followed the protocol published elsewhere ([19]). DETD-3 was derived from DET by translactonization via the hydrolysis of DET followed by acidic treatment. DETD-5, −6, −13, −17, −19, −24, −31, −33, −35, −39, and −43 were further synthesized from DETD-3 ([26]).

Chemicals and reagents

3-(4,5-Dimethylthiazol-2-yl)-2,5-diphenyltetrazolium bromide (MTT), dimethyl sulfoxide (DMSO), *N*-acetyl-*L*-cysteine (NAC) and crystal violet were purchased from Sigma-Aldrich (St. Louis, MO). DMEM, fetal bovine serum (FBS), and the antibiotic mixture (penicillin-streptomycin) were from Invitrogen (Carlsbad, CA, USA). PLX4032 and MEK inhibitor (PD0325901) were purchased from Selleck Chemical (Houston, TX). All other solvents or chemicals were of reagent or HPLC grade.

Cell lines and culture conditions

Normal human epithelial cell melanocytes (ATCC® PCS-200-012™) and a spectrum of wild-type or mutant melanoma cell lines including murine B16-F10 (ATCC® CRL-6475™): NRAS mutation and human cell lines MeWo (ATCC® HTB-65™): wild-type, A375 (ATCC® CRL-1619™) and A2058 (ATCC® CRL-11147™): $BRAF^{V600E}$ mutation, and SK-MEL-2 (ATCC® HTB-68™): NRAS mutation were obtained from the ATCC (Manassas, VA). All cell lines were purchased during 2010–2012 and authenticated originally by ATCC using short tandem repeat (STR) analysis. Cells were expanded and frozen down at low

passage within 1 month after the receipt of the original stocks. Cells were then thawed and used within 15 passages without further authentication for this study. Cells were cultured in manufacturers' suggested medium supplemented with 10% fetal bovine serum, 100 units/mL penicillin, and 100 μg/mL streptomycin at 37 °C in a humidified 5% CO_2 incubator.

Animals

Female NOD/SCID mice bred in the Laboratory Animal Core Facility (Agricultural Biotechnology Research Center, Academia Sinica, Taiwan) were given a standard laboratory diet and distilled H_2O *ad libitum* and kept on a 12 h light/dark cycle at 22±2 °C. All experimental protocols (No: 11-02-137) were approved by the Institutional Animal Care and Utilization Committee, Academia Sinica, Taiwan.

Cell viability assay

Cells were seeded in 96-well plates overnight and treated with compounds for 24 to 72 h. Cell growth was determined by MTT-based colorimetric assays according to Scudiero *et al.* ([27]). Viability of the cells treated with vehicle-only (0.5% DMSO) was defined as 100% viability. Survival of cells after treatment with compound or PLX4032 were calculated using the following formula: viable cell number (%) = [OD_{570} (treated cell culture)/OD_{570} (vehicle control)] × 100.

Compound-drug combination assay

Concentrations of DETD-35 and PLX4032 for compound-drug combination study were selected based on their IC_{50} values from MTT assay. The Chou-Talalay method was used to determine the effects of a compound-drug combination on A375 cells ([28]). The interaction of DETD-35 and PLX4032 was determined by the combination index (CI), and the CI plot was generated using CompuSyn software. The combined effects of two compounds can be categorized as follows: CI < 1 indicates synergism; CI = 1 indicates an additive effect; CI > 1 indicates antagonism between the two compounds tested ([28]).

Colony formation assay

Colony-forming cell growth was obtained by growing A375 or A375-R cells in 24-well plates with indicated treatments for 21 days. The medium containing the compound or drug was refreshed every three days. Cell colonies were stained with 0.1% (w/v) crystal violet in phosphate buffer saline, dried and photographed. Cell-retained crystal violet was extracted with 20% (v/v) acetic acid in water and quantitatively measured by absorbance at 595 nm. Relative colony-forming percentage in each treatment was compared to the control treatment.

Cell cycle analysis

Cell cycle analysis was performed as described by Shyur *et al.* ([29]). Cells were synchronized by incubation in medium containing 1% FBS for 12 h, and the culture was then incubated with fresh medium/10% FBS containing vehicle or compound for 24 h. Both adherent and floating cells were collected, washed with PBS and fixed with 1 mL of ice-cold 70% ethanol

overnight at 4°C. Cells were stained with propidium iodide/RNase A solution for 30 minutes at room temperature in the dark and then analyzed by flow cytometry (Flow cytometer BD LSR II).

Apoptosis detection

Cells were seeded in 6-well plates and treated with vehicle or indicated compounds. After 72 h of incubation, apoptotic cells were analyzed using FITC Annexin V Apoptosis Detection Kit (BD Pharmingen) according to the manufacturer's instructions and flow cytometry.

Western blot analysis

Total cellular proteins were prepared from tested cells as previously described ([30]). Protein concentration was determined by the Bradford method (Bio-Rad). Protein samples were resolved by 5% to 20% gradient SDS-PAGE and then underwent immunoblotting. Primary antibodies against ERK1/2 (Sc-94), Bax (Sc-20067), Akt (Sc-5298), JNK (Sc-571), c-Jun (Sc-1694) and STAT3 (Sc-482) were purchased from Santa Cruz Biotechnology, phospho-Src (GTX81151) was purchased from GeneTex, Src (2778-1) was purchased from Epitomics, phospho-Akt (#4058), phospho-STAT3 (#9131), phospho-MEK (#9121), MEK (#9122), phospho-ERK1/2 (#9106), p27 (#2552), cyclin D1 (#2978), BcL-xL (#2764), phospho-SAPK/JNK (#9251), phospho-c-Jun (#9261), caspase 7 (#9492), cleaved caspase 7 (#9491), PARP (#9542), and cleaved PARP (#5625) were purchased from Cell Signaling Technology, and actin (MAB1501) was purchased form Merck Millipore. Appropriate horseradish peroxidase-conjugated secondary antibodies were used. Protein bands reacting to specific antibodies were visualized by use of enhanced chemiluminescence (Amersham) with exposure to chemiluminescence light film (BioMax; Kodak Co.). The resulting images were quantified by densitometry using Bio-Profil (Bio-1D 97.04, Vilber-Lourmat).

Caspase-3 activity assay

Caspase-3 activity was detected using NucView 488 Caspase-3 Assay Kit for Live Cells (Biotium, Catalog No. 30029). Briefly, A375 and A375-R cells were seeded in 10 cm plates, treated with vehicle or compound for 72 h, and then the cells were trypsinized and resuspended at a density of 1×10^6 cells/mL. Cell suspension (0.2 mL) was pipetted into a test tube and incubated with a 5 μM NucView 488 substrate concentration for 30 min at room temperature in the dark. After that, 300 μL of PBS was added into each test tube and analyzed by flow cytometry. The intensity of the fluorescence was measured at an excitation wavelength of 485 nm and an emission wavelength of 515 nm.

Measurement of reactive oxygen species (ROS)

ROS level in the cells was measured using Total ROS Detection Kit (Enzo, Catalog No. 51011). Briefly, A375 and A375-R cells were seeded in 10 cm plates for 18 h. Cells were pretreated with or without 5 mM NAC for 1 h before treating with vehicle or compounds for 2 h. The cells were then trypsinized and resuspended in 500 μL of ROS detection solution which can be reacted to a wide range of reactive species, such as hydrogen peroxide, peroxynitrite, hydroxyl radicals, nitric oxide and peroxy radical, yielding a green fluorescent

product, and incubated for 30 min at 37 °C. The generated ROS level was then analyzed by flow cytometry.

In vivo xenograft tumor models

A375, A375-R or A2058 cells (3×10^6) were injected subcutaneously to the flanks of 6-week-old NOD/SCID mice. Once the tumor volume reached around 50 mm^3, the mice were randomized into treatment groups ($n = 8$ per group) and the treatments were started. Body weight and tumor volume of the mice were recorded every three days using formula $a \times b^2 \times 0.5$, where a and b represent the larger and smaller tumor diameters ([31]). Tumor growth inhibition (TGI) was calculated as $100 \times [1 - (\text{mean tumor volume final} - \text{mean tumor volume initial})_{\text{treatment group}}/(\text{mean tumor volume final} - \text{mean tumor volume initial})_{\text{vehicle group}}]$ ([31]).

Immunohistochemistry analysis

The formalin-fixed and paraffin-embedded tumor sections (4 μm thick) were heat immobilized and deparaffinized with xylene and rehydrated in a graded series of ethanol with a final wash in distilled water. Antigen retrieval involved use of Target Retrieval Solution (DakoCytomation, Glostrup, Denmark) in a Decloaking Chamber (Biocare Medical, Walnut Creek, CA). The following antibodies were used for immunohistochemistry analysis: phospho-Src (GTX81151) from GeneTex, phospho-Akt (#4060), phospho-MEK (#2338), phospho-ERK1/2 (#4370), Ki-67 (#9027), cleaved caspase-3 (#9661), and cleaved PARP (#5625) from Cell Signaling Technology.

Statistical analysis

Data are expressed as mean ± SEM. Statistical analyses were conducted using an SAS program (SAS Institute), and significant differences within treatments were determined by ANOVA. P values of less than 0.05 were considered statistically significant.

Results

DET and DETDs inhibit melanoma cell proliferation *in vitro*

DET had an anti-proliferative effect on human A375 or mouse B16-F10 melanoma cells at an IC_{50} value of 6.0 μM; however, the re-lactonized derivative DETD-3 did not show anti-melanoma cell proliferation activity within the same tested concentration up to 10 μM (Table 1). Thus, the hydroxyl group at the C-6 position in DETD-3 was further modified to improve the activity and/or study the structure-activity relationship. Attaching an acyl group on the C-6 hydroxyl group can produce an ester, which may act not only as a prodrug, but also influence the interaction of the drug. An additional acyl group might provide an H-bond acceptor, of appropriate size to fill in the cavity space of the protein binding site, with decent hydrophobicity, and so on. The aliphatic groups of various sizes were connected to produce DETD-17, −5, −13, −19, and −24. An aromatic group offers a planarity and π-electron rich space, which may play an important role in ligand-protein interaction. Therefore, benzoyl, phenyl acetoxyl, and cinnamoyl groups were also connected to the C-6 hydroxyl to produce DETD-31, −33, −43, −35, −6 and −39, respectively. These ester derivatives could have

various distances between the aromatic ring and the terpene skeleton. Chemical structures of DET and DETDs are shown in Table 1.

All synthesized DETDs together with the parental phytocompound DET as a reference were evaluated for anti-melanoma cell proliferation activity using wild-type as well as mutant melanoma cell lines B16-F10, MeWo, A375, A2058, SK-MEL-2, and normal melanocytes. DET only inhibited B16-F10 and A375 cell proliferation, but showed no detectable activities against other human melanoma cells at tested concentrations up to 10 μM. Among DETDs with aliphatic ester groups, only DETD-5 showed comparable antiproliferative activities against the tested melanoma cells, except wild-type MeWo and normal melanocytes, with IC_{50} values of 4.1–7.8 μM. Other aliphatic ester derivatives, such as DETD-17, −13, −19, and −24, did not show inhibitory effects on any of the tested human melanoma cells. Compared to aliphatic ester derivatives, interestingly, most DETDs with the aromatic ester group inhibited the melanoma cell growth without affecting normal cells. Aromatic ester derivatives, DETD-33, −35, −6 and −39, inhibited all tested melanoma cell proliferation with IC_{50} values of 3.9–9.9, 2.2–6.7, 2.5–6.0, and 1.6–3.5 μM, respectively. Particularly, DETD-35 with 10π electronic naphthalene group and DETD-39 with 3-methoxycinnamate group demonstrated two times more potent anti-proliferation against the tested melanoma cells than DET itself. These results indicate that the feature of the aromatic ring on the ester group is favored for the anti-melanoma activity and more electron rich systems tend to be more potent. DETD-39 is slightly cytotoxic to normal human melanocytes with an IC_{50} of 9.0 μM (Table 1), while DETD-35 was demonstrated to have little or no toxicity to normal melanocytes, with only 9.1% inhibition detected at 10 μM concentration. Therefore, we chose DETD-35 for further investigation.

DETD-35 shows synergism with vemurafenib in inhibiting A375 cell proliferation

Compound-drug combination assay was carried out to evaluate the potential synergism between vemurafenib and DETD-35. The MTT-based anti-proliferation assay showed that the IC_{50} of PLX4032 and DETD-35 on A375 cells were 0.07 and 0.85 μM, respectively, when 2×10^3 cells were initially seeded and treated with the compound for 72 h (Fig. 1A and B). A greater dose-dependent cytotoxicity of DETD-35 to A375 cells was observed at the tested compound concentrations up to 20 μM in which less than 10% viable cells were detected (data not shown). MTT assay with a fixed concentration of PLX4032 (10 nM) combined with increasing concentrations of DETD-35 (0.1 to 1 μM) showed better inhibition compared to DETD-35 treatment alone at the same tested concentrations (Fig. 1C). The CI values calculated using CalcuSyn software for combination treatment of DETD-35 and vemurafenib were within 0.60 to 1.05, indicating either synergism or an additive effect of the compound-drug combination (Fig. 1D).

We also evaluated the long-term anti-proliferative effects of DETD-35 and PLX4032 (treatment for 21 days) using colony formation assay. The parental compound DET was also evaluated in parallel. PLX4032 inhibited colony formation of A375 cells, with 55% inhibition at 0.1 μM treatment. DETD-35 or DET alone also showed inhibition in a dose-dependent manner. Of note, cells treated with DETD-35 at 0.5 μM, 1.25 μM and 2.5 μM inhibited 42%, 71% and 98% colony formation, respectively, and 1 μM, 2.5 μM and 5 μM of

DET treatment inhibited 38%, 65% and 91% colony formation, respectively, of A375 cells. Importantly, the combination treatment displayed better effects than the individual compound or drug treatment. At 0.1 μM PLX4032 plus 1.25 μM DETD-35 or 2.5 μM DET, the inhibition reached 88% and 81%, respectively (Fig. 1E). The anti-proliferative effect of PLX4032 was strongly associated with induction of G_1-phase cell-cycle arrest (Fig. 2F). DETD-35 did not have any significant effect on A375 DNA distribution in the cell-cycle, while DET at 5 μM induced G_2/M-phase arrest (Fig. 1F). Both DETD-35 and DET treatment induced high levels of A375 cell apoptosis, up to 85.2% and 67.8%, respectively; however, PLX4032 treatment only induced 10.4% apoptosis in the cells (Fig. 1G). We found that the profound effect of PLX4032 on inducing G_1-phase cell-cycle arrest dominated the effect of compound (DETD-35 or DET)-drug combination in A375 cells, whereas DETD-35 or DET-sensitized PLX4032 induced A375 cell apoptosis to 91% and 69%, respectively (Fig. 1F and G).

DETD-35 deregulates MEK-ERK signaling and induces apoptotic hallmarks in A375 cells

Next, we investigated the underlying mechanisms by which DET, DETD-35 and PLX4032 inhibited A375 melanoma cell activity. We observed that PLX4032 inhibited MEK and ERK phosphorylation, increased p27 expression and suppressed cyclin D1 expression as shown by western blotting (Fig. 2A). DETD-35 or DET also inhibited MEK and ERK phosphorylation, but had no effect on p27 and cyclin D1 expression; however, both compounds induced the apoptotic hallmarks, the cleaved form of PARP accumulation and caspase-3 activity in the cells (Fig. 2A and B). The compound-drug combination showed inhibition of pMEK, pERK and cyclin D1 expression as well as induction of p27 and cleaved PARP protein levels (Fig. 2A), and caspase-3 activity (Fig. 2B), indicating combination treatment integrated the effects of PLX4032 and DET or DETD-35 in A375 cells. Other apoptotic markers Bax and BcL-xL were not responsive to PLX4032, DET or DETD-35 treatment.

DETD-35 alone or in combination with vemurafenib suppresses tumor growth in an A375 orthotopic xenograft model

We used an A375 human melanoma xenograft model to further evaluate the *in vivo* bioefficacy of DET, DETD-35, PLX4032 and the compound-drug combination. Supplementary Figure S1A displays the detailed experimental design for A375 xenograft study. Figure 3A shows representative tumor tissues from the tumor control and treatment groups of the A375 xenograft study. PLX4032 (20 mg/kg/day, 24 doses in total) was effective in suppressing tumor growth with 87.4% tumor growth inhibition (TGI) and reduction of tumor mass by 71.9%. We observed that DETD-35 and DET (20 mg/kg/every two days, 12 doses in total) also suppressed tumor growth with 87.1% and 71.0% TGI and reduced tumor mass by 70.5% and 47.5%, respectively (Fig. 3B and C), indicating DETD-35 was as effective as vemurafenib and possessed better anti-melanoma growth activity than DET. Importantly, the compound-drug combination in which DETD-35 (20 mg/kg/every four days, 6 doses in total) and PLX4032 (20 mg/kg/every two days, 12 doses in total) were administered alternately and the treatment frequency was only half of the single compound administration frequency, showed similar anti-tumor efficacy as the single agent treatment (91.0% TGI and 72.3% reduction in tumor mass), suggesting synergism of

DETD-35 and PLX4032 in mice (Fig. 3B and C). In addition, there were no indications of toxicity such as body weight loss or changes in organ index in the treatment groups (Supplementary Fig. S1B and C). Immunohistochemical analysis showed PLX4032 significantly inhibited pMEK, pERK and proliferation marker Ki-67 levels, and slightly induced the apoptotic markers, i.e., cleaved caspase-3 and cleaved PARP levels in the tumor tissues (Fig. 3D). We observed that DETD-35 and DET also significantly inhibited pMEK, pERK and Ki-67 levels in which the inhibitory effect of DETD-35 was significantly better than DET (Fig. 3D). Moreover, both compounds showed stronger induction of cleaved caspase-3 and cleaved PARP levels compared to PLX4032 treatment. Importantly, we found that the compound-drug combination reduced levels of pMEK, pERK and Ki-67 as did PLX4032 and induced levels of cleaved caspase-3 and cleaved PARP as did DETD-35 (Fig. 3D). These results were in good agreement with results observed in the *in vitro* studies.

DETD-35 overcomes acquired vemurafenib resistance *in vitro*

To study whether or not DETD-35 could overcome acquired resistance to BRAF inhibitor in A375 cells, we first generated the A375 cell line which was resistant to PLX4032 (A375-R) as previously reported ([10]). Briefly, A375 melanoma cells were seeded in T75 plates and treated with increasing concentrations of PLX4032 (10, 20, 50, 100, 250, 500, 1000, 2000, 5000 nM) through approximately 2 months and 20 passages. We have successfully developed acquired resistance cell line A375-R which is 100-fold less sensitive to PLX4032 treatment compared to parental cell line (IC_{50}: 7.34 vs. 0.07 μM). Importantly, DETD-35 and DET were still effective against the resistance cell line (Fig. 4A, B and C). PLX4032 revealed no inhibitory effect on colony formation whereas DETD-35 and DET inhibited colony formation of A375-R cells in a dose dependent manner (Fig. 4D). Moreover, the compound-drug combination showed dramatic inhibition of A375-R cell colony formation, indicating DETD-35 or DET could sensitize the anti-proliferative effect of PLX4032 (Fig. 4D). Consistent with the anti-proliferation results, PLX4032 had no effect on cell-cycle distribution and apoptosis of A375-R cells. DETD-35 had no effect on cell-cycle distribution whereas DET caused G_2/M-phase cell-cycle arrest in A375-R cells. Furthermore, both DET and DETD-35 induced high-levels of (86∼89%) apoptosis in A375-R cells (Supplementary Fig. S2A and B). For mechanistic studies, we included MEK inhibitor combined with PLX4032 as a positive control since MEKi combination with vemurafenib is used to treat $BRAF^{V600E}$ melanoma patients clinically ([16]). We found that PLX4032 inhibited pSrc, pMEK, pERK, pAkt and pSTAT3 protein levels in A375 cells. In contrast, phosphoproteins were reactivated in PLX4032-treated A375-R cells. Moreover, PLX4032 could not induce p27 expression or reduce cyclin D1 level in A375-R cells, in the same as observed in PLX4032-treated A375 cells (Fig. 4E). DETD-35 and DET, however, could suppress the phosphorylated proteins, suggesting inhibition of their reactivation in resistant A375 cells. Both compounds were also observed to induce cleaved PARP expression and caspase-3 activity in A375-R cells (Fig. 4E and Supplementary Fig. S2C). Compound-drug combination with DETD-35 or DET plus PLX4032 also inhibited levels of pSrc, pMEK, pERK, pAkt and pSTAT3 proteins, in the same way as the MEK inhibitor+PLX4032 (Fig. 4E). Interestingly, the compound-drug combination induced cleaved PARP expression whereas MEK inhibitor+PLX4032 treatment induced p27 expression and reduced cyclin D1 expression (Fig. 4E).

DETD-35 overcomes acquired and intrinsic vemurafenib resistance *in vivo*

We used A375-R (acquired vemurafenib resistance) and A2058 (intrinsic vemurafenib resistance due to lack of PTEN expression) xenograft mouse models to evaluate the *in vivo* bioefficacy of DETD-35, DET, PLX4032 and the compound-drug combination against vemurafenib resistance melanoma. Supplementary Figure S3A displays the detailed experimental design for A375-R and A2058 xenograft study. Figure 5A shows representative tumor tissues from the A375-R xenograft study. PLX4032 treatment (75 mg/kg/day, 24 doses in total) showed no anti-tumor activity with similar tumor growth rate and sizes compared to the tumor control group in both A375-R (Fig. 5B and C) and A2058 (Fig. 5D and E) xenograft models, as expected. DETD-35 (20 mg/kg/every two days, 12 doses in total) effectively inhibited A375-R (Fig. 5B and C) and A2058 (Fig. 5D and E) tumor growth in mice with 47.1% and 73.7% TGI and a reduction in tumor mass of 46.3% and 69.0%, respectively. DET (20 mg/kg/every two days, 12 doses in total) only inhibited A375-R tumors with 31.2% TGI (Fig. 5B). Notably, the compound-drug combination in which alternate administration of DETD-35 (20 mg/kg/every two days, 12 doses in total) and PLX4032 (75 mg/kg/every two days, 12 doses in total) showed the best anti-tumor activity in both vemurafenib resistance xenografts A375-R (Fig. 5B and C) and A2058 (Fig. 5D and E), with 76.5% and 79.0% TGI and 65.2% and 75.3% reduction in tumor mass, respectively. There was no indication of toxicity such as body weight loss or organ index changes in the treatment groups (Supplementary Fig. S3B, C, D and E). Consistent with *in vitro* studies, immunohistochemical analyses showed that DETD-35 and DET treatment or the compound-drug combination significantly reduced pSrc, pMEK, pERK, pAKt and Ki-67 levels, and increased cleaved caspase-3 and cleaved PARP levels in A375-R xenograft tissues, but PLX4032 alone did not have effect on the expression of these proteins (Fig. 5F). Notably, DETD-35 showed more activity than DET, a result which mirrored the observations in the A375 xenograft study.

DETD-35 induces generation of reactive oxygen species (ROS) to trigger apoptotic cell death in A375 and A375-R cells

Previously, we demonstrated that DET treatment can induce oxidative stress to facilitate the activation of the c-Jun N-terminal kinase (JNK) signaling pathway towards apoptotic cell death in TS/A cells ([19]). We evaluated whether DETD-35 exerts the same mechanism by inducing ROS-mediated apoptosis in A375 and A375-R cells. We first performed the proliferation assay in the cells with or without pretreatment with the ROS scavenger NAC. As shown in Figure 6, the 1 μM DETD-35 and 2 μM DET treatment inhibited 59% and 55% A375 cell viability and 69% and 65% A375-R cell viability, respectively, and 5 mM NAC alone did not affect either type of cell viability (Fig. 6A and B). However, treatment with NAC for 1 h before treating with either DET or DETD-35 restored cell viability in both A375 and A375-R cells (Fig. 6A and B), suggesting that the presence of ROS is correlated to the inhibitory effect of DET or DETD-35 on melanoma cell viability. We then examined the ROS levels in the cells treated with DET or DETD-35 using flow cytometry. Treatment with 2.5 μM DETD-35 or 5 μM DET for 2 h significantly increased (more than 2-fold) ROS level in both A375 and A375-R cells, as indicated by the data in Fig. 6C; this effect could be significantly reversed by pretreating the cells with 5 mM NAC for 1 h (Fig. 6C). Because oxidative stress can activate JNK, which subsequently induces c-Jun activation and

phosphorylation to trigger apoptosis in cancer cells ([19]), we thus further analyzed JNK signaling molecules in the cells with the same treatment by western blotting. We observed that DETD-35 significantly activated p-c-Jun and c-Jun protein levels at early time points (2, 4 and 8 h) in both A375 and A375-R cells, and less effect was observed for the DET treatment (Fig. 6D). Furthermore, cell apoptosis markers, cleaved forms of caspase-7 (cl-caspase-7) and PARP (cl-PARP), were strongly induced by DETD-35 and DET treatment at a later treatment time point (24 h) in both A375 and A375-R cells (Fig. 6D). Notably, pretreatment with 5 mM NAC for 1 h significantly blockaded DETD-35-induced cascade protein expression or activation of p-c-Jun/c-Jun, cl-caspase-7 and cl-PARP in both cell lines. Interestingly, although DET was also observed to induce ROS production in both cell lines and the significant DET-induced apoptosis could be also reversed by NAC pretreatment, the activation of p-c-Jun/c-Jun was found much less significant compared to that of DETD-35. Together, our results indicate that DETD-35 or DET induced apoptotic cell death in A375 and A375-R cells were in part through generation of ROS, yet different pathways might be involved in both compound effects.

Discussion

From the early 1980s to 2010, dacarbazine was the only FDA-approved chemotherapeutic drug for the treatment of metastatic melanoma with 15% to 20% overall response, 4 to 6 month of medium response duration, and less than 5% complete response ([32]). However, management of melanoma has improved dramatically in recent years. For example, the immunotherapeutic agent ipilimumab which acts against cytotoxic T-lymphocyte-associated protein 4 (CTLA-4), and targeted therapeutics agents such as vemurafenib and dabrafenib (BRAF inhibitor) show a remarkable tumor response rate and prolong patient survival leading to a new era of melanoma therapies ([33]). Unfortunately, melanoma tumors frequently relapse due to acquired drug resistance to both immunotherapeutics and targeted therapeutics agents; consequently, there is a growing and urgent need to develop novel or alternative therapeutic approaches for cutaneous melanoma. In this study, we created a phytocompound derivative DETD-35 and demonstrated that it possessed a better effect than the parental natural compound DET on inhibiting the proliferation of a panel of melanoma cells with different genetic backgrounds. *In vitro* mechanistic studies suggested that DETD-35 acted through inducing cell apoptosis while vemurafenib mainly caused G_1-phase cell cycle arrest in A375 cells. Notably, treatment with a combination of DETD-35 and vemurafenib not only induced apoptosis (increased in cleaved PARP expression and caspase-3 activity) but also caused G_1-phase cell cycle arrest (increased p27 expression and suppressed cyclin D1 expression) in A375 cells. These data suggest the synergistic or complementary effect of the compound-drug combination, resulting in better inhibitory effects on colony formation and induction of more significant apoptosis in melanoma cells compared to compound or drug treatment alone. When anti-tumor growth activity was evaluated *in vivo* in parallel with FDA approved drug vemurafenib against $BRAF^{V600E}$ mutant melanoma, DETD-35 showed comparable bioefficacy. Furthermore, the compound-drug combination showed statistically similar *in vivo* bioefficacy as a single compound treatment in which the treatment frequency of the compound-drug combination was only

half of the single compound administration frequency. These data suggested that DETD-35 possesses both therapeutic and adjuvant activity against $BRAF^{V600E}$ mutant melanoma.

Resistance to vemurafenib therapy is mainly due to reactivation of MEK-ERK signaling in cells. In addition, activated RTK-driven alternative mechanisms such as the PI3K-Akt survival pathway also contributed to resistance to vemurafenib ([9]). Furthermore, Girotti and colleagues recently showed that EGFR-SRC family kinase (SFK)-STAT3 signaling is upregulated in vemurafenib resistant cells ([34]). Consistent with those previous studies, we showed the reactivation of phosphorylated forms of Src, MEK, ERK, Akt and STAT-3 in our in-house established resistance cell line A375-R. DETD-35 inhibited the reactivation of the proteins in the resistance cells in the same way as observed with the positive control MEK inhibitor. Interestingly, we observed that MEKi overcame acquired vemurafenib resistance by restoring the expression of p27 and inhibiting cyclin D1 that led to G_1-phase cell-cycle arrest in the cells. In contrast, DETD-35 displayed a different mechanism to the MEK inhibitor, sensitizing vemurafenib to inhibit proliferative capability and enhance apoptosis of A375-R cells in xenograft mice. Moreover, DETD-35 also sensitized vemurafenib to inhibit intrinsic resistance tumor (A2058 xenograft) growth in mice. These data indicated the novel effect of DETD-35 in circumvention of both acquired and intrinsic vemurafenib resistant melanoma growth in mice.

Recent studies have shown multiple vemurafenib resistance mechanisms between patients, within patients and even within the same tumor biopsy ([35], [36]). It is therefore anticipated that multiple pathway inhibition combined with vemurafenib will achieve durable clinical control of $BRAF^{V600E}$ melanoma ([35], [36]). In our study, we showed that DETD-35 could deregulate multiple signaling molecules including MEK-ERK, Akt, and STAT3 in vemurafenib resistant melanoma cells A375-R, as shown in the schematic model (Supplementary Fig. S4), which supports, at least in part, the novel pharmacological activity of the new compound DETD-35. The complementary and synergistic activities of DETD-35 and vemurafenib against $BRAF^{V600E}$ mutant melanoma and acquired vemurafenib resistance melanoma growth in mice suggested a novel strategy for the management of late stage $BRAF^{V600E}$ melanoma by using DETD-35 as a direct therapy or an adjuvant agent of vemurafenib.

Supplementary Material

Refer to Web version on PubMed Central for supplementary material.

Acknowledgments

We thank Dr. Yu-Chuan Liang and Laboratory Animal Core Facility of Agricultural Biotechnology Research Center, Academia Sinica, Taiwan for the experimental NOD/SCID mice.

Financial Support

This work was supported by a Grant from Ministry of Science and Technology (MOST 103-2320-B-001-008-MY3), Taiwan and institutional grant awarded to L.F. Shyur. This study was also supported in part by a Grant-in-Aid from the Ministry of Education, Culture, Sports, Science and Technology (MEXT KAKENHI, Japan) awarded to K. Nakagawa-Goto. (Grant Number 25293024 & 25670054), and a NIH grant from the National Cancer Institute awarded to K.H. Lee (CA-177584).

References

1. Greenlee RT, Hill-Harmon MB, Murray T, Thun M. Cancer statistics, 2001. CA Cancer J Clin. 2001; 51:15–36. [PubMed: 11577478]
2. Siegel RL, Miller KD, Jemal A. Cancer statistics, 2015. CA Cancer J Clin. 2015; 65:5–29. [PubMed: 25559415]
3. Halilovic E, Solit DB. Therapeutic strategies for inhibiting oncogenic BRAF signaling. Curr Opin Pharmacol. 2008; 8:419–426. [PubMed: 18644254]
4. Tsai J, Lee JT, Wang W, Zhang J, Cho H, Mamo S, et al. Discovery of a selective inhibitor of oncogenic BRAF kinase with potent antimelanoma activity. Proc Natl Acad Sci U S A. 2008; 105:3041–3046. [PubMed: 18287029]
5. Chapman PB, Hauschild A, Robert C, Haanen JB, Ascierto P, Larkin J, et al. Improved survival with vemurafenib in melanoma with $BRAF^{V600E}$ mutation. N Engl J Med. 2011; 364:2507–2516. [PubMed: 21639808]
6. Shi H, Moriceau G, Kong X, Lee MK, Lee H, Koya RC, et al. Melanoma whole-exome sequencing identifies $BRAF^{V600E}$ amplification-mediated acquired BRAF inhibitor resistance. Nat Commun. 2012; 3:724. [PubMed: 22395615]
7. Nazarian R, Shi H, Wang Q, Kong X, Koya RC, Lee H, et al. Melanomas acquire resistance to $BRAF^{V600E}$ inhibition by RTK or NRAS upregulation. Nature. 2010; 468:973–977. [PubMed: 21107323]
8. Johannessen CM, Boehm JS, Kim SY, Thomas SR, Wardwell L, Johnson LA, et al. COT drives resistance to RAF inhibition through MAP kinase pathway reactivation. Nature. 2010; 468:968–972. [PubMed: 21107320]
9. Villanueva J, Vultur A, Lee JT, Somasundaram R, Fukunaga-Kalabis M, Cipolla AK, et al. Acquired resistance to BRAF inhibitors mediated by a RAF kinase switch in melanoma can be overcome by cotargeting MEK and IGF-1R/PI3K. Cancer Cell. 2010; 18:683–695. [PubMed: 21156289]
10. Yadav V, Zhang X, Liu J, Estrem S, Li S, Gong XQ, et al. Reactivation of mitogen-activated protein kinase (MAPK) pathway by FGF receptor 3 (FGFR3)/Ras mediates resistance to vemurafenib in human $BRAF^{V600E}$ mutant melanoma. J Biol Chem. 2012; 287:28087–28098. [PubMed: 22730329]
11. Straussman R, Morikawa T, Shee K, Barzily-Rokni M, Qian ZR, Du J, et al. Tumour micro-environment elicits innate resistance to RAF inhibitors through HGF secretion. Nature. 2012; 487:500–504. [PubMed: 22763439]
12. Solit DB, Rosen N. Resistance to BRAF inhibition in melanomas. N Engl J Med. 2011; 364:772–774. [PubMed: 21345109]
13. Vergani E, Vallacchi V, Frigerio S, Deho P, Mondellini P, Perego P, et al. Identification of MET and SRC activation in melanoma cell lines showing primary resistance to PLX4032. Neoplasia. 2011; 13:1132–1142. [PubMed: 22241959]
14. Chapman PB. Mechanisms of resistance to RAF inhibition in melanomas harboring a BRAF mutation. Am Soc Clin Oncol Educ Book. 2013
15. Lito P, Pratilas CA, Joseph EW, Tadi M, Halilovic E, Zubrowski M, et al. Relief of profound feedback inhibition of mitogenic signaling by RAF inhibitors attenuates their activity in $BRAF^{V600E}$ melanomas. Cancer Cell. 2012; 22:668–682. [PubMed: 23153539]
16. Curti BD. Rapid evolution of combination therapy in melanoma. N Engl J Med. 2014; 371:1929–1930. [PubMed: 25390744]
17. Smyth T, Paraiso KH, Hearn K, Rodriguez-Lopez AM, Munck JM, Haarberg HE, et al. Inhibition of HSP90 by AT13387 delays the emergence of resistance to BRAF inhibitors and overcomes resistance to dual BRAF and MEK inhibition in melanoma models. Mol Cancer Ther. 2014; 13:2793–2804. [PubMed: 25349308]
18. Flaherty KT, Infante JR, Daud A, Gonzalez R, Kefford RF, Sosman J, et al. Combined BRAF and MEK inhibition in melanoma with $BRAF^{V600E}$ mutations. N Engl J Med. 2012; 367:1694–1703. [PubMed: 23020132]

19. Huang CC, Lo CP, Chiu CY, Shyur LF. Deoxyelephantopin, a novel multifunctional agent, suppresses mammary tumour growth and lung metastasis and doubles survival time in mice. Br J Pharmacol. 2010; 159:856–871. [PubMed: 20105176]
20. Huang CC, Lin KJ, Cheng YW, Hsu CA, Yang SS, Shyur LF. Hepatoprotective effect and mechanistic insights of deoxyelephantopin, a phyto-sesquiterpene lactone, against fulminant hepatitis. J Nutr Biochem. 2013; 24:516–530. [PubMed: 22748804]
21. Lee WL, Wen TN, Shiau JY, Shyur LF. Differential proteomic profiling identifies novel molecular targets of paclitaxel and phytoagent deoxyelephantopin against mammary adenocarcinoma cells. J Proteome Res. 2010; 9:237–253. [PubMed: 19894775]
22. Lee WL, Shyur LF. Deoxyelephantopin impedes mammary adenocarcinoma cell motility by inhibiting calpain-mediated adhesion dynamics and inducing reactive oxygen species and aggresome formation. Free Radic Biol Med. 2012; 8:1423–1436. [PubMed: 22342517]
23. Kabeer FA, Sreedevi GB, Nair MS, Rajalekshmi DS, Gopalakrishnan LP, Kunjuraman S, et al. Antineoplastic effects of deoxyelephantopin, a sesquiterpene lactone from *Elephantopus scaber*, on lung adenocarcinoma (A549) cells. J Integr Med. 2013; 11:269–277. [PubMed: 23867245]
24. Su M, Chung HY, Li Y. Deoxyelephantopin from *Elephantopus scaber* L. induces cell-cycle arrest and apoptosis in the human nasopharyngeal cancer CNE cells. Biochem Biophys Res Commun. 2011; 411:342–347. [PubMed: 21741953]
25. Geetha BS, Nair MS, Latha PG, Remani P. Sesquiterpene lactones isolated from *Elephantopus scaber* L. inhibits human lymphocyte proliferation and the growth of tumour cell lines and induces apoptosis *in vitro* . J Biomed Biotechnol. 2012; 2012:721285. [PubMed: 22500104]
26. Nakagawa-Goto K, Chen JY, Cheng YT, Lee YL, Takeya M, Saito Y, et al. Novel sesquiterpene lactone analogues as potent anti-breast cancer agents. Article in press (Mol Oncol). 2016
27. Scudiero DA, Shoemaker RH, Paull KD, Monks A, Tierney S, Nofziger TH, et al. Evaluation of a soluble tetrazolium/formazan assay for cell growth and drug sensitivity in culture using human and other tumor cell lines. Cancer Res. 1988; 48:4827–4833. [PubMed: 3409223]
28. Chou TC. Drug combination studies and their synergy quantification using the Chou-Talalay method. Cancer Res. 2010; 70:440–446. [PubMed: 20068163]
29. Shyur LF, Chen CH, Lo CP, Wang SY, Kang PL, Sun SJ, et al. Induction of apoptosis in MCF-7 human breast cancer cells by phytochemicals from *Anoectochilus formosanus* . J Biomed Sci. 2004; 11:928–939. [PubMed: 15591790]
30. Chiang YM, Lo CP, Chen YP, Wang SY, Yang NS, Kuo YH, et al. Ethyl caffeate suppresses NFκB activation and its downstream inflammatory mediators, iNOS, COX-2, and PGE2 *in vitro* or in mouse skin. Br J Pharmacol. 2005; 146:352–363. [PubMed: 16041399]
31. Yang H, Higgins B, Kolinsky K, Packman K, Go Z, Iyer R, et al. RG7204 (PLX4032), a selective $BRAF^{V600E}$ inhibitor, displays potent antitumor activity in preclinical melanoma models. Cancer Res. 2010; 70:5518–5527. [PubMed: 20551065]
32. Hsan KM, Chen CC, Shyur LF. Current research and development of chemotherapeutic agents for melanoma. Cancers (Basel). 2010; 2:397–419. [PubMed: 24281076]
33. Michielin O, Hoeller C. Gaining momentum: New options and opportunities for the treatment of advanced melanoma. Cancer Treat Rev. 2015; 41:660–670. [PubMed: 26096079]
34. Girotti MR, Pedersen M, Sanchez-Laorden B, Viros A, Turajlic S, Niculescu-Duvaz D, et al. Inhibiting EGF receptor or SRC family kinase signaling overcomes BRAF inhibitor resistance in melanoma. Cancer Discov. 2013; 3:158–167. [PubMed: 23242808]
35. Rizos H, Menzies AM, Pupo GM, Carlino MS, Fung C, Hyman J, et al. BRAF inhibitor resistance mechanisms in metastatic melanoma: spectrum and clinical impact. Clin Cancer Res. 2014; 20:1965–1977. [PubMed: 24463458]
36. Van Allen EM, Wagle N, Sucker A, Treacy DJ, Johannessen CM, Goetz EM, et al. The genetic landscape of clinical resistance to RAF inhibition in metastatic melanoma. Cancer Discov. 2014; 4:94–109. [PubMed: 24265153]

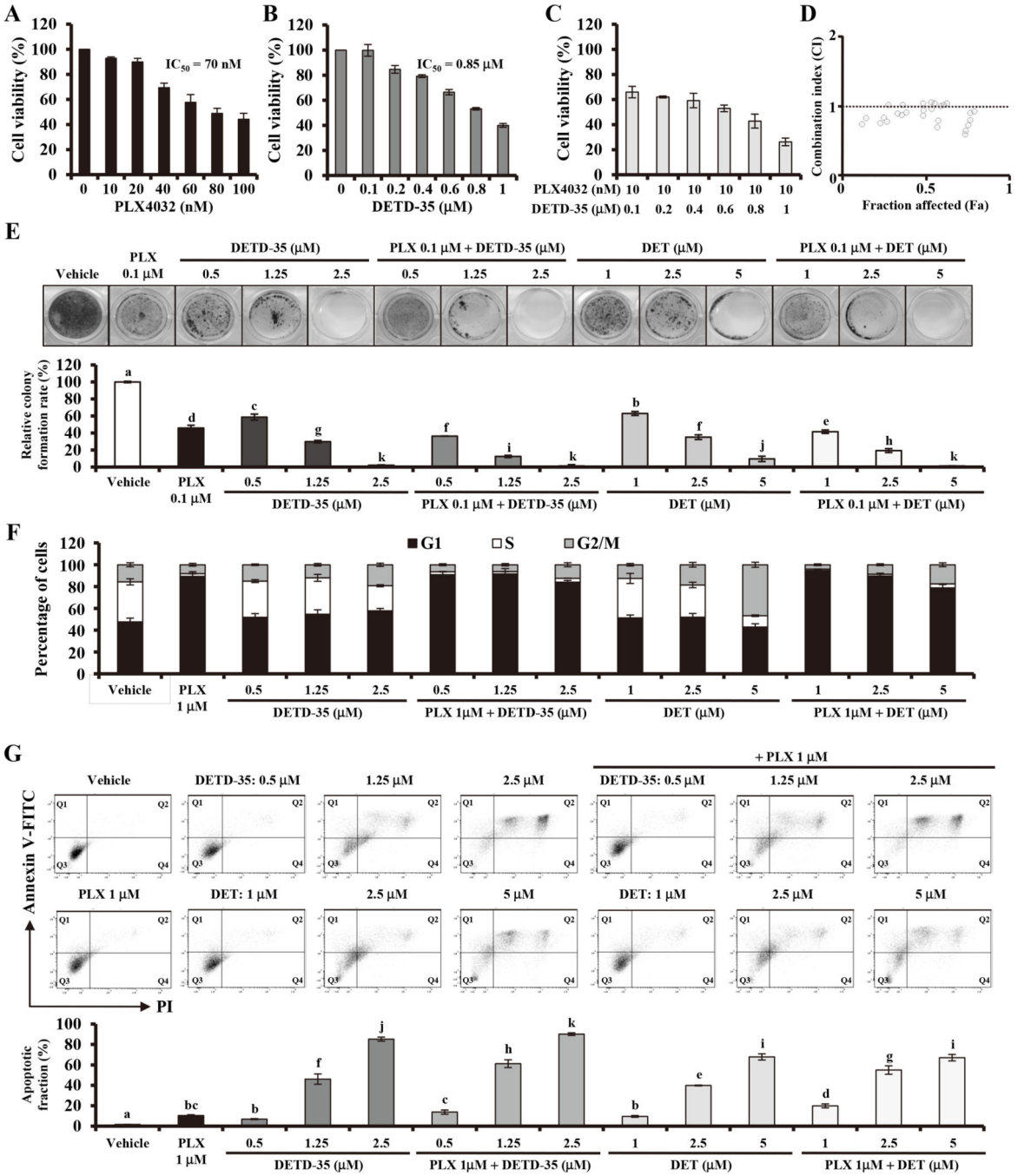

Figure 1.

DETD-35 shows synergism with vemurafenib *in vitro*. A, B and C, A375 melanoma cells were treated with the indicated concentrations of PLX4032, DETD-35 and PLX4032***35 for 72 h, respectively. Cell viability was determined using MTT assay. D, compound-drug combination study using CalcuSyn software. CI < 1 indicates synergism; CI = 1 indicates additive effect; CI > 1 indicates antagonism between the two compounds tested. E, top: colony formation assay showing long-term (21-day treatment) anti-proliferative effects of PLX4032, DETD-35 and DET against A375 cells. Crystal violet stained cells are shown.

Bottom: quantification of the crystal violet absorbance at 595 nm after 21 days of treatment. Data are mean ± SEM, $n = 4$. Means without a common letter differ, $P < 0.05$. F, cell-cycle analysis, cells were treated with the indicated concentrations of compounds for 24 h. After fixation, cells were stained with propidium iodide and analyzed by flow cytometry. G, combination of DETD-35 or DET with PLX4032 increased levels of apoptosis in A375 melanoma cells. Cells were treated with the indicated concentrations of the compounds for 72 h. Apoptosis status in cells was measured by Annexin V/FITC plus propidium iodide double staining and flow cytometry. Top: Representative quadrant diagrams showing cell distribution in Q1 (early apoptosis), Q2 (apoptosis), Q3 (live), and Q4 (dead). Bottom: apoptotic fraction was calculated by adding distribution percentage in Q1, Q2 and Q4 together. Data are mean ± SEM, $n = 3$. Means without a common letter differ, $P < 0.05$.

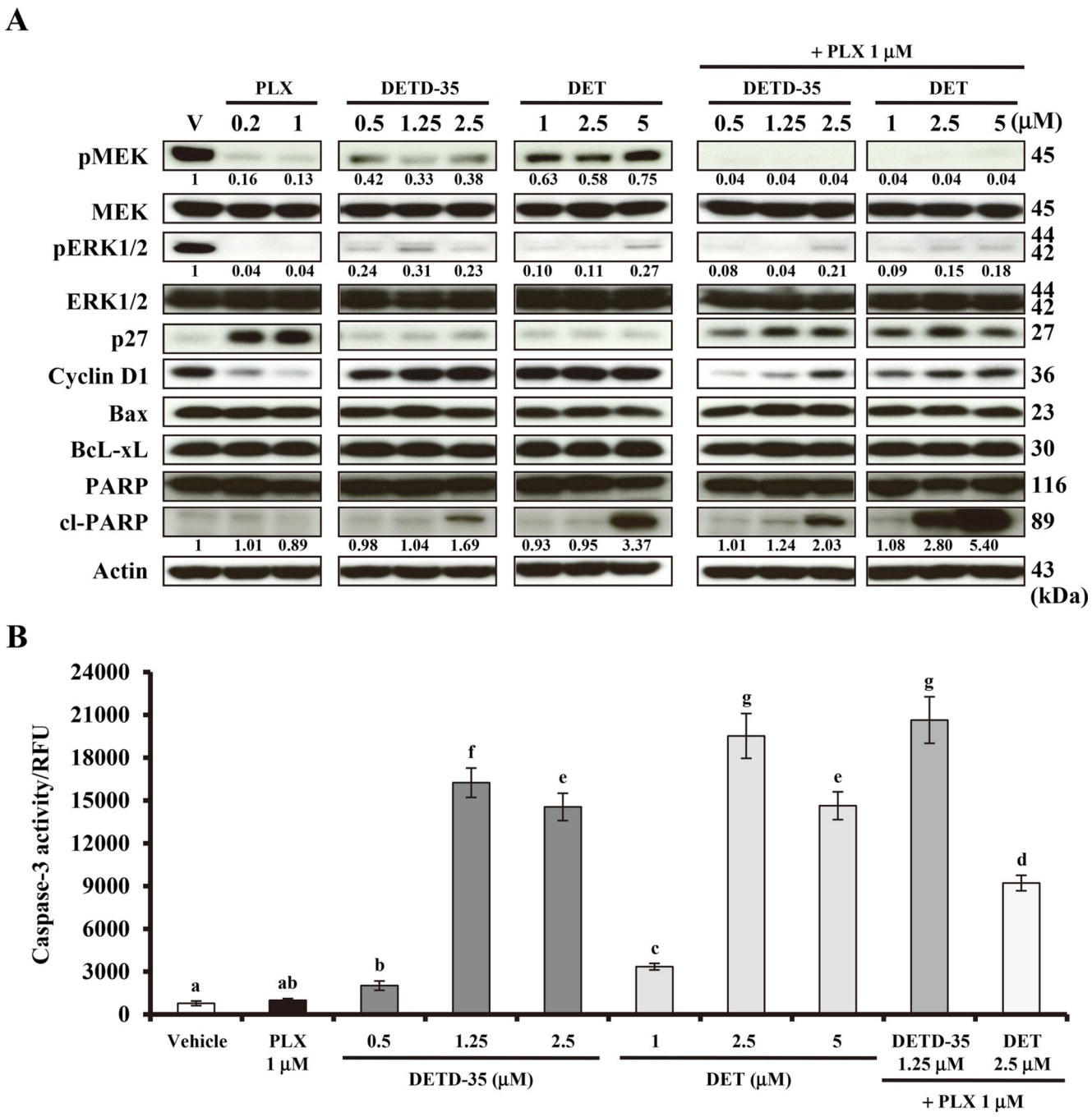

Figure 2.

DETD-35 suppresses MEK-ERK signaling and induces apoptosis in A375 melanoma cells. A, cells were treated with indicated concentrations of the compounds for 16 h before lysis. Cell lysates were subjected to western blotting against the specific antibodies indicated, and actin was used as an internal or loading control. Quantification of specific protein expression, which was normalized to actin first followed by comparison of the fold-change within different treatments to vehicle treatment. B, cells were treated with indicated concentrations of the compounds for 72 h, caspase 3 activity was determined by measuring

cleavage of a fluorogenic substrate using flow cytometry (RFU: relative fluorescence units). Data are mean ± SEM, $n = 3$. Means without a common letter differ, $P < 0.05$.

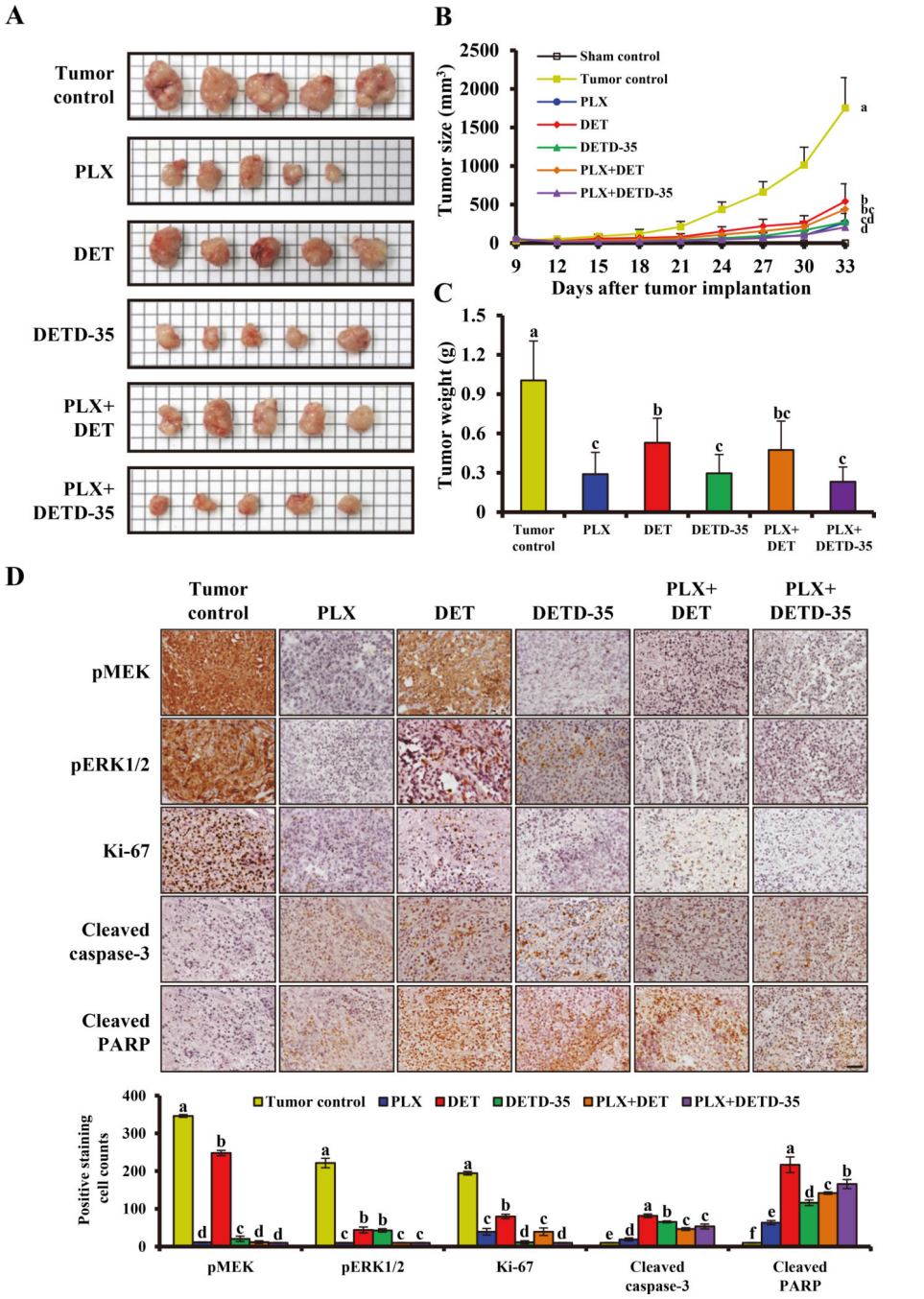

Figure 3.

DETD-35 inhibits $BRAF^{V600E}$ mutant melanoma growth *in vivo*. NOD/SCID mice bearing A375 xenografts were treated with vehicle, PLX4032 (20 mg/kg/day), DETD-35 or DET (20 mg/kg/every two days), and a compound-drug combination with alternate administration of DETD-35 or DET (20 mg/kg/every four days) plus PLX4032 (20 mg/kg/every two days), when tumor volume reached around 50 mm^3. A, representative tumor tissues isolated from each treatment group. B, tumor volume was measured every three days and plotted as mean ± SEM. C, the weight of the dissected tumors from each treatment group. Data are mean ±

SEM, $n = 8$. Means without a common letter differ, $P < 0.05$. D, top: representative immunohistochemistry images of tumor tissues with positive staining of phospho-MEK, phospho-ERK1/2, Ki-67, cleaved caspase-3 and cleaved PARP (brownish color) and nuclear (blue color) by hematoxylin staining are shown (Scale bar: 50 μm). Bottom: quantification of phospho-MEK, phospho-ERK1/2, Ki-67, cleaved caspase-3 and cleaved PARP positive stained cells, Data are mean ± SEM, $n = 3$. Means without a common letter differ, $P < 0.05$.

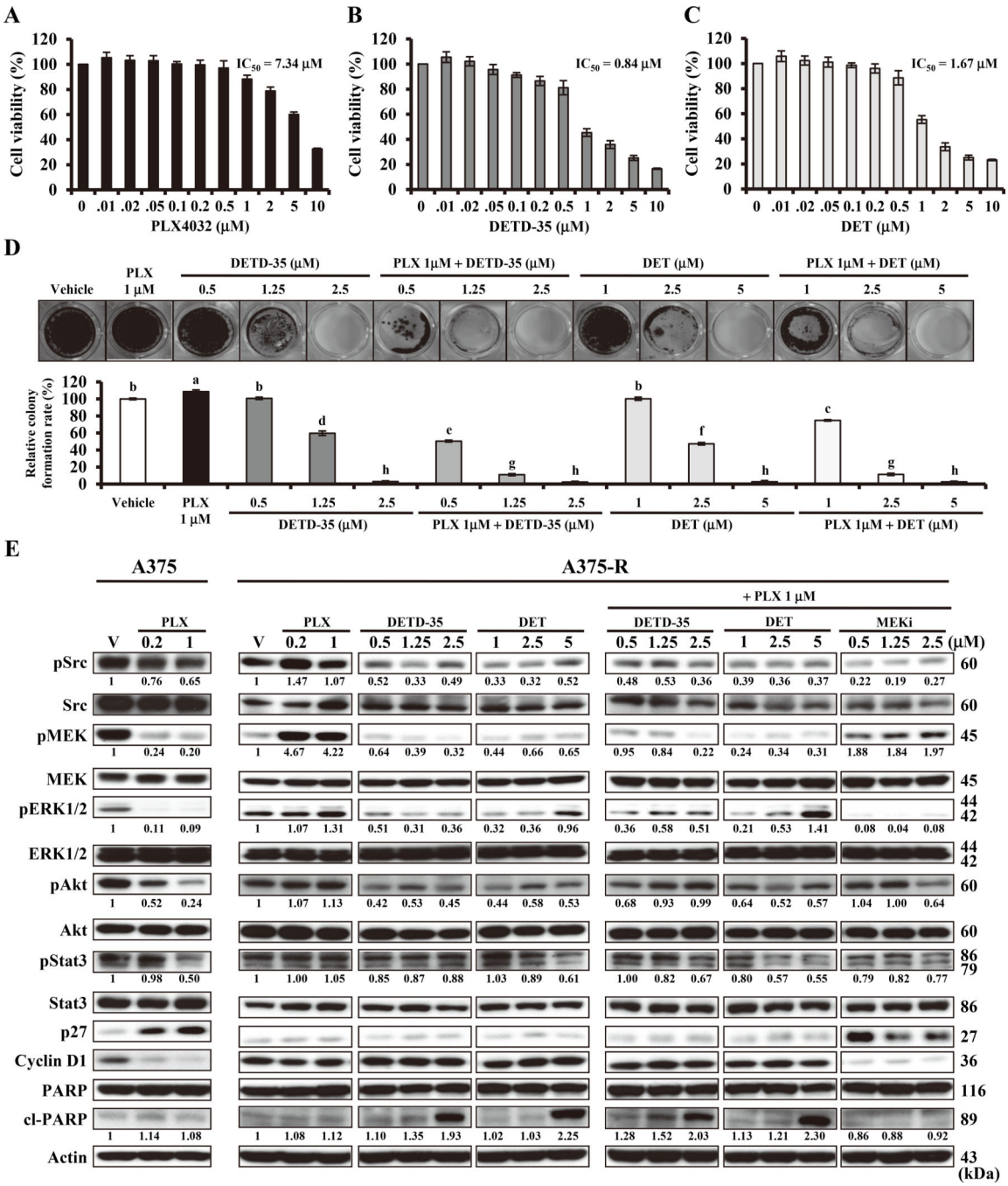

Figure 4.

DETD-35 overcomes acquired vemurafenib resistance *in vitro*. A, B and C, A375-R cells were treated with indicated concentrations of PLX4032, DETD-35 and DET for 72 h. Cell viability was determined using MTT assay. D, top: colony formation assay showing long-term (21-day treatment) anti-proliferative effects of PLX4032, DETD-35 and DET against A375-R cells. Crystal violet stained cells are shown. Bottom: quantification of the crystal violet absorbance at 595 nm after 21 days of treatment. Data are mean ± SEM, $n = 4$. Means without a common letter differ, $P < 0.05$. E, A375-R cells were treated with the indicated

concentrations of compounds for 16 h before lysis. Cell lysates were subjected to western blotting using the specific antibodies indicated, and actin was used as an internal or loading control. Quantification of specific protein expression, which was normalized to actin first followed by comparison of the fold change within different treatments to vehicle treatment.

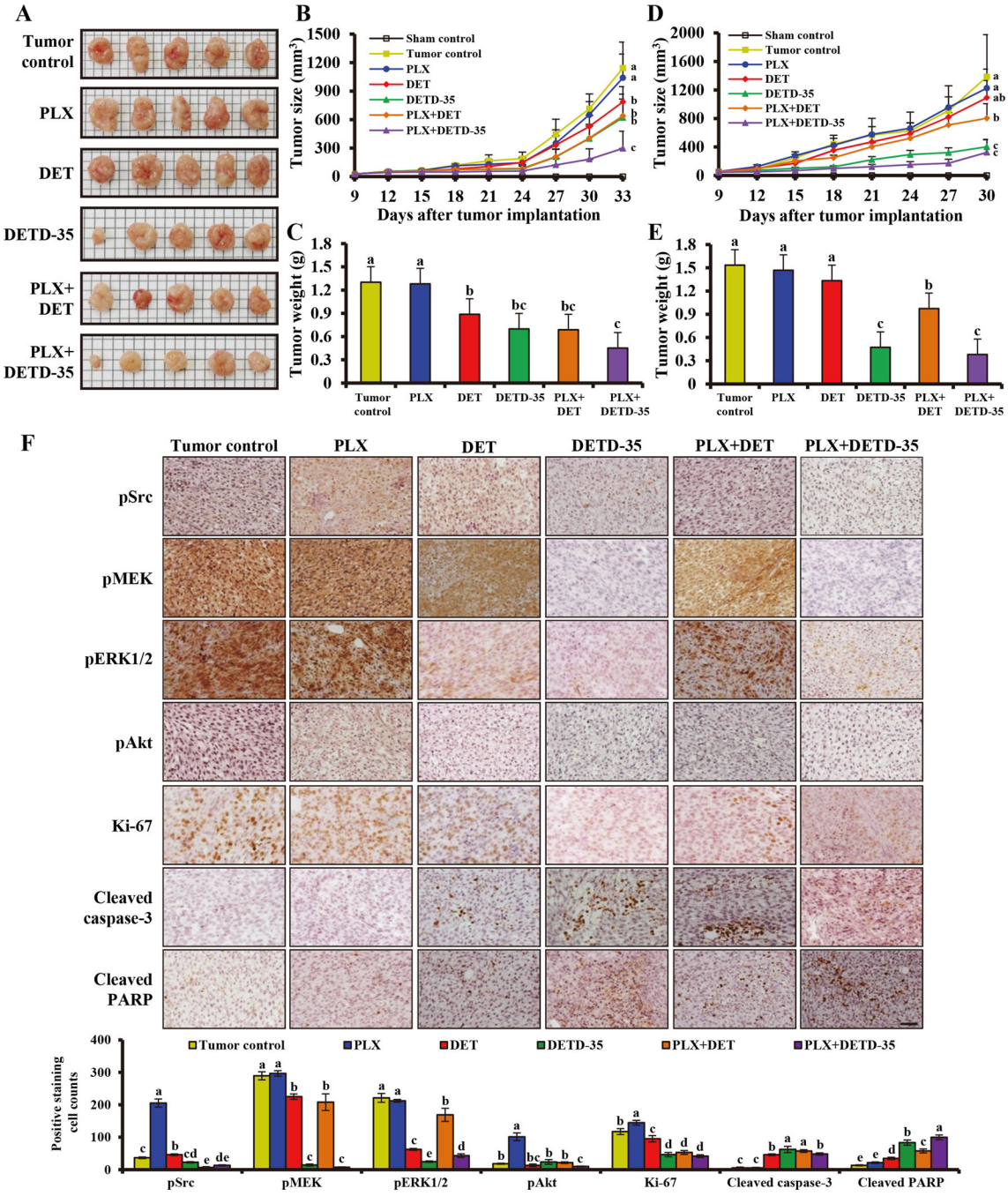

Figure 5.

DETD-35 overcomes both intrinsic and acquired vemurafenib resistance in mice. NOD/SCID mice bearing A375-R and A2058 xenografts were treated with vehicle, PLX4032 (75 mg/kg/day), DETD-35 or DET (20 mg/kg/every two days), and a compound-drug combination with alternate administration of DETD-35 or DET (20 mg/kg/every two days) and PLX4032 (75 mg/kg/every two days), when tumor volume reached around 50 mm^3. A, representative tumor tissues isolated from A375-R xenograft. B, tumor volume of A375-R xenograft was measured every three days and plotted as mean ± SEM. C, the weight of the

dissected tumors from A375-R xenograft. D, tumor volume of A2058 xenograft was measured every three days and plotted as mean ± SEM. E, the weight of the dissected tumors from A2058 xenograft. Data are mean ± SEM, $n = 8$. Means without a common letter differ, $P < 0.05$. F, top: representative immunohistochemistry images of A375-R tumor for positive staining of phospho-Src, phospho-MEK, phospho-ERK1/2, phospho-Akt, Ki-67, cleaved caspase-3, and cleaved PARP (Scale bar: 50 μm). Bottom: quantification of phospho-Src, phospho-MEK, phospho-ERK1/2, phospho-Akt, Ki-67, cleaved caspased-3, and cleaved PARP positive stained cells from tumor tissue sections of A375-R xenograft study. Data are mean ± SEM, $n = 3$. Means without a common letter differ, $P < 0.05$.

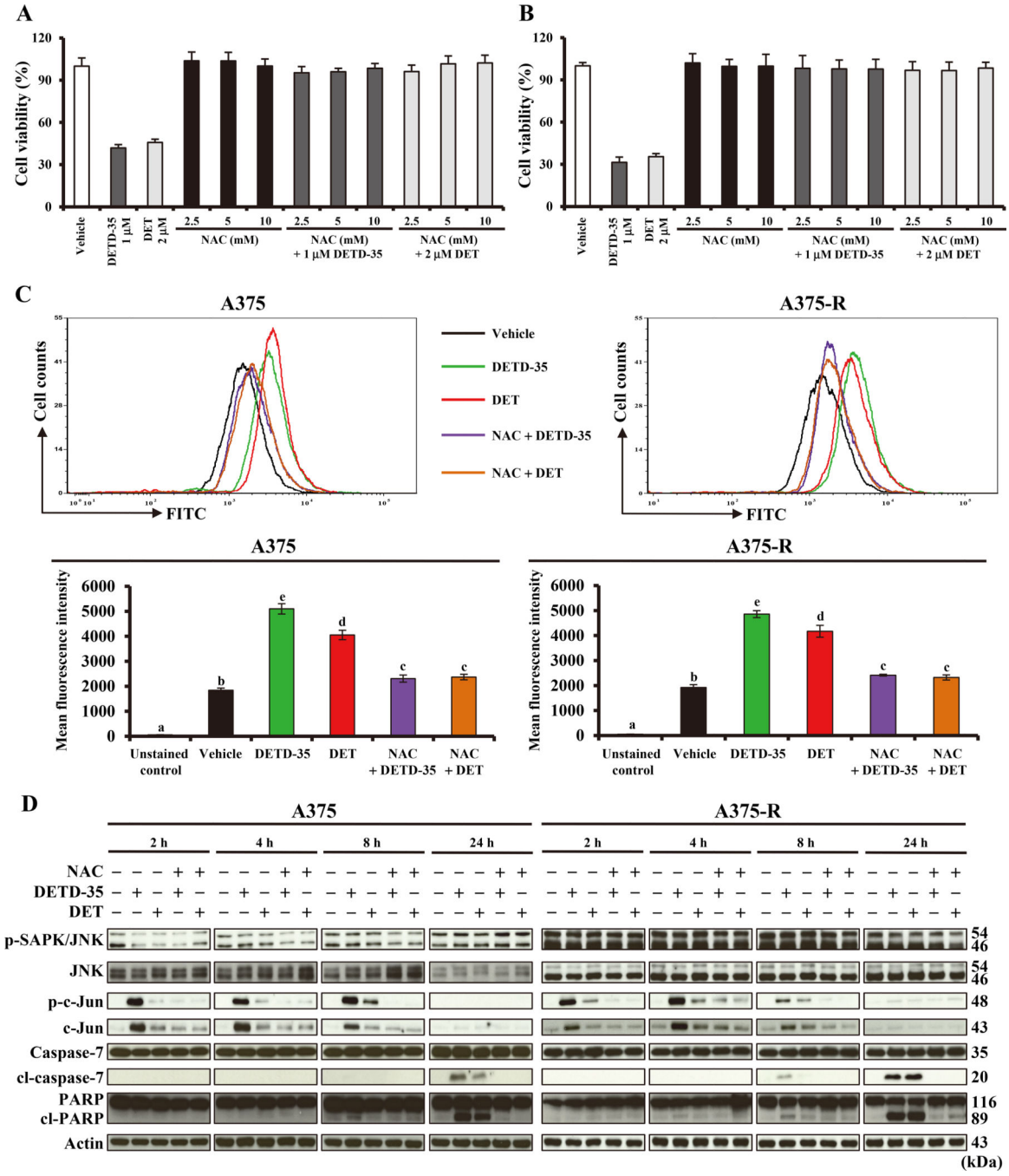

Figure 6.

DETD-35 induces oxidative stress to trigger apoptosis in A375 and A375-R cells. A and B, A375 cells and A375-R cells, respectively, were pretreated with or without NAC for 1 h followed by treatment with DETD-35 or DET at the indicated concentrations for 72 h. Cell viability was determined using MTT assay. C, top: reactive oxygen species (ROS) generation in A375 cells and A375-R cells treated with DETD-35 and DET alone or pretreated with NAC for 1 h followed by compound treatment for 2 h. Flow cytometry and green fluorescent dye (ROS detection probe) were used in this experiment. Bottom:

quantification of the generated ROS in the cells under the same treatment as top panel. Data are mean ± SEM, $n = 4$. Means without a common letter differ, $P < 0.05$. D, cell lysates from A375 and A375-R cells pretreated with or without NAC for 1 h followed by treatment with 2.5 μM DETD-35 and 5 μM DET at the indicated times were collected and subjected to western blotting using the specific antibodies indicated, and actin was used as an internal or loading control.

Mol Cancer Ther. Author manuscript; available in PMC 2017 June 01.

Table 1

Structure of DET and its derivatives (DETDs) and their effects on proliferation of different melanoma cell lines and normal melanocytes.[a]

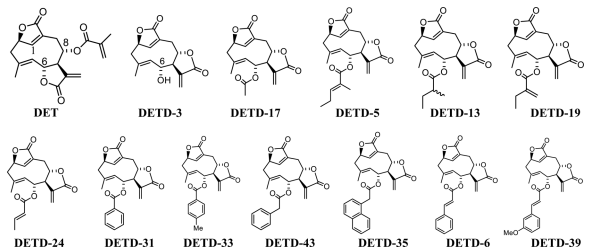

Compound	B16-F10[b] (NRAS mutation)	MeWo[c] (No NRAS or BRAF mutation)	SK-MEL-2[c] (NRAS mutation)	A2058[c] (BRAF mutation)	A375[c] (BRAF mutation)	Melanocyte[c] (Normal cells)
DET	6.0 ± 0.13	-	-	-	5.9 ± 0.55	-
DETD-3	-	-	-	-	-	-
DETD-17	-	-	-	-	-	-
DETD-5	4.7 ± 0.03	-	7.8 ± 0.14	5.8 ± 0.08	4.1 ± 0.15	-
DETD-13	7.1 ± 0.09	-	-	-	-	-
DETD-19	7.8 ± 0.28	-	-	-	-	-
DETD-24	-	-	-	-	-	-
DETD-31	2.9 ± 0.78	-	-	-	4.3 ± 0.62	-
DETD-33	2.2 ± 0.29	6.7 ± 0.22	5.9 ± 0.20	4.2 ± 0.09	2.9 ± 0.26	-
DETD-43	7.4 ± 0.48	-	8.2 ± 0.27	8.7 ± 0.33	3.6 ± 0.25	-
DETD-35	2.7 ± 0.09	6.0 ± 0.37	3.9 ± 0.07	3.1 ± 0.19	2.5 ± 0.23	-
DETD-6	3.9 ± 0.18	9.9 ± 0.05	5.7 ± 0.17	3.9 ± 0.09	3.3 ± 0.22	-
DETD-39	1.7 ± 0.18	3.5 ± 0.30	3.2 ± 0.27	2.4 ± 0.15	1.6 ± 0.14	9.0 ± 0.57

[a]The cells were treated with DET and its derivatives for 24 h, and the numbers in the table are the 50% inhibitory concentration (IC_{50} in μM) of each compound.

[b]mouse cell line.

[c]human cell line.

IC_{50} is not detectable at the measured concentrations up to 10 μM.